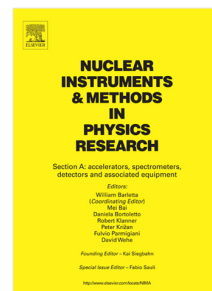


Accepted Manuscript

HERMES: An ultra-wide band X and gamma-ray transient monitor on board a nano-satellite constellation

F. Fuschino, R. Campana, C. Labanti, Y. Evangelista, M. Feroci, L. Burderi, F. Fiore, F. Ambrosino, G. Baldazzi, P. Bellutti, R. Bertacin, G. Bertuccio, G. Borghi, D. Cirrincione, D. Cauz, F. Ficorella, M. Fiorini, M. Gandola, M. Grassi, A. Guzman, G. La Rosa, M. Lavagna, P. Lunghi, P. Malcovati, G. Morgante, B. Negri, G. Pauletta, R. Piazzolla, A. Picciotto, S. Pirrotta, S. Pliego-Caballero, S. Puccetti, A. Rachevski, I. Rashevskaya, L. Rignanese, M. Salatti, A. Santangelo, S. Silvestrini, G. Sottile, C. Tenzer, A. Vacchi, G. Zampa, N. Zampa, N. Zorzi



PII: S0168-9002(18)31681-4
DOI: <https://doi.org/10.1016/j.nima.2018.11.072>
Reference: NIMA 61613

To appear in: *Nuclear Inst. and Methods in Physics Research, A*

Received date: 3 July 2018
Revised date: 9 November 2018
Accepted date: 13 November 2018

Please cite this article as: F. Fuschino, R. Campana, C. Labanti et al., HERMES: An ultra-wide band X and gamma-ray transient monitor on board a nano-satellite constellation, *Nuclear Inst. and Methods in Physics Research, A* (2018), <https://doi.org/10.1016/j.nima.2018.11.072>

This is a PDF file of an unedited manuscript that has been accepted for publication. As a service to our customers we are providing this early version of the manuscript. The manuscript will undergo copyediting, typesetting, and review of the resulting proof before it is published in its final form. Please note that during the production process errors may be discovered which could affect the content, and all legal disclaimers that apply to the journal pertain.

1 NIMA POST-PROCESS BANNER TO BE
2 REMOVED AFTER FINAL ACCEPTANCE

3 HERMES: An ultra-wide band X and gamma-ray
4 transient monitor on board a nano-satellite
5 constellation

6 F. Fuschino^{a,b,*}, R. Campana^{a,b}, C. Labarini^{a,b}, Y. Evangelista^{c,d}, M. Feroci^{c,d},
7 L. Burderi^e, F. Fiore^h, F. Ambrosio^c, G. Baldazzi^{e,b}, P. Bellutti^q,
8 R. Bertacin^r, G. Bertuccio^{m,n}, C. Longini^q, D. Cirrincione^{i,k}, D. Cauzi^{i,j},
9 F. Ficorella^q, M. Fiorini^f, M. Gardola^{m,n}, M. Grassi^o, A. Guzman^t,
10 G. La Rosa^s, M. Lavagna^p, P. Lunghi^p, P. Malcovati^o, G. Morgante^a,
11 B. Negri^r, G. Pauletta^j, R. Piazzolla^c, A. Picciotto^q, S. Pirrotta^r,
12 S. Pliego-Caballero^t, S. Puccetti^r, A. Rachevski^k, I. Rashevskaya^l,
13 L. Rignanese^{e,b}, M. Salatti^r, L. Santangelo^t, S. Silvestrini^p, G. Sottile^s,
14 C. Tenzer^t, A. Vacchi^l, G. Zampa^k, N. Zampa^k, N. Zorzi^q

15 ^aINAF-CAS Fognano, Via Gobetti 101, I-40129 Bologna, Italy

16 ^bINFN sez. Bologna, Viale Berti-Pichat 6/2, I-40127 Bologna, Italy

17 ^cINAF-IAPS, Via del Fosso del Cavaliere 100, I-00133 Rome, Italy

18 ^dINFN sez. Roma 2, Via della Ricerca Scientifica 1, I-00133 Rome, Italy

19 ^eUniversity of Bologna, Dep. of Physics and Astronomy - DIFA, viale Berti Pichat 6/2,
20 I-40127 Bologna, Italy

21 ^fINAF-IASF Milano, Via Bassini 15, I-20100 Milano, Italy

22 ^gUniversity of Cagliari, Dep. of Physics, S.P. Monserrato-Sestu Km 0,700, I-09042
23 Monserrato (CA), Italy

24 ^hINAF-OATs Via G.B. Tiepolo, 11, I-34143 Trieste

25 ⁱUniversity of Udine, Via delle Scienze 206, I-33100 Udine, Italy

26 ^jINFN Udine, Via delle Scienze 206, I-33100 Udine, Italy

27 ^kINFN sez. Trieste, Padriciano 99, I-34127 Trieste, Italy

28 ^lTIFPA-INFN, Via Sommarive 14, I-38123 Trento, Italy

29 ^mPolitecnico di Milano, Department of Electronics, Information and Bioengineering, Via
30 Anzani 42, I-22100 Como, Italy

31 ⁿINFN sez. Milano, Via Celoria 16, I-20133 Milano, Italy

32 ^oUniversity of Pavia, Department of Electrical, Computer, and Biomedical Engineering,
33 and INFN Sez. Pavia, Via Ferrata 3, I-27100 Pavia, Italy

34 ^pPolitecnico di Milano, Bovisa Campus, Via La Masa 34 - I-20156 Milano, Italy

*Corresponding author

Email address: fuschino@iasfbo.inaf.it (F. Fuschino)

35 ^aFondazione Bruno Kessler – FBK, Via Sommarive 18, I-38123 Trento, Italy
36 ^rItalian Space Agency - ASI, Via del Politecnico snc, 00133 Roma, Italy
37 ^sINAF/IASF Palermo, Via Ugo La Malfa 153, I-90146 Palermo, Italy
38 ^tUniversity of Tübingen-IAAT, Sand 1, D-72076 Tübingen, Germany

39 **Abstract**

The High Energy Modular Ensemble of Satellites (HERMES) project is aimed to realize a modular X/gamma-ray monitor for transient events, to be placed on-board of a nano-satellite bus (e.g. CubeSat). This expandable platform will achieve a significant impact on Gamma-Ray Burst (GRB) science and on the detection of Gravitational Wave (GW) electromagnetic counterparts: the recent LIGO/VIRGO discoveries demonstrated that the high-energy transient sky is still a field of extreme interest. The very complex temporal variability of GRBs (experimentally verified up to the millisecond scale) combined with the spatial and temporal coincidence between GWs and their electromagnetic counterparts suggest that upcoming instruments require sub-microsecond time resolution combined with transient localization accuracy lower than a degree. The current phase of the ongoing HERMES project is focused on the realization of a technological Pathfinder with a small network (3 units) of nano-satellites to be launched in mid 2020. We will show the potential and prospects for short and medium-term development of the project, demonstrating the disrupting possibilities for scientific investigations provided by the innovative concept of a new “modular astronomy” with nano-satellites (e.g. low developing costs, very short realization time). Finally, we will illustrate the characteristics of the HERMES Technological Pathfinder project, demonstrating how the scientific goals discussed are actually already reachable with the first nano-satellites of this constellation. The detector architecture will be described in detail, showing that the new generation of scintillators (e.g. GAGG:Ce) coupled with very performing Silicon Drift Detectors (SDD) and low noise Front-End-Electronics (FEE) are able to extend down to few keV the sensitivity band of the detector. The technical solutions for FEE, Back-End-Electronics (BEE) and Data

Handling will be also described.

40 *Keywords:* Nanosatellites, Gamma-ray Burst, Silicon Drift Detectors,
41 Scintillator Detectors

42 *PACS:* 95.55.Ka, 29.40.Wk, 29.40.Mc,

43 1. Introduction

44 Gamma-Ray Bursts (GRBs) are one of the most intriguing and challeng-
45 ing phenomena for modern science. Their study is of very high interest for
46 several fields of astrophysics, such as the physics of matter in extreme condi-
47 tions and black holes, cosmology, fundamental physics and the mechanisms of
48 gravitational wave signal production, because of their huge luminosities, up to
49 more than 10^{52} erg/s, their red-shift distribution extending from $z \sim 0.01$ up to
50 $z > 9$ (i.e., much above that of supernovae of the Ia class and galaxy clusters),
51 and their association with peculiar core-collapse supernovae and with neutron
52 star/black hole mergers.

53 Since their discovery, GRBs were promptly identified as having a non-terrestrial
54 origin [1]. First observations were done using radiation monitors onboard the
55 VELA spacecraft constellation, that was a network of satellites designed to mon-
56 itor atmospheric nuclear tests. Between 1963 and 1970 a total of 12 satellites
57 were launched and the constellation was operating until 1985, with more sen-
58 sitive detectors on later satellites. By analyzing the different arrival times of
59 the γ -ray photon bursts as detected by different satellites, placed in different
60 locations around the Earth, it was possible to roughly estimate the direction
61 of the GRB, later improved using additional and better detectors, reaching a
62 precision of $\sim 10^\circ$. With a very similar approach, the Inter-Planetary Network
63 (IPN¹, including all satellites with GRB-sensitive instruments on-board) was
64 organised by GRB scientists in late '70s, aiming to localize GRBs for the ob-
servation of counterparts at other wavelengths. Basing on the availability of

¹<https://heasarc.gsfc.nasa.gov/w3browse/all/ipngrb.html>

66 operating instruments, the IPN in its lifetime has involved up to more than 20
67 different spacecrafts. This experience demonstrates that the localization accu-
68 racy of GRBs is improved by increasing the spacing between different detectors,
69 and also by a more accurate detector timing resolution. The IPN localizations
70 are usually provided in few days, and although can reach angular resolutions of
71 arcminutes and often arcseconds, the current typical accuracy, at high energies,
72 is of the order of few degrees. This was demonstrated, e.g., in the case of the
73 discovery of Gravitational Wave (GW) electromagnetic counterparts [2]. Such
74 huge error box is too large to be efficiently surveyed at optical wavelengths,
75 where tens/hundreds of optical transient sources are usually found, increasing
76 enormously the probability to find spurious correlations. The best strategy here
77 is to perform a prompt search for transients at high energies, with a localiza-
78 tion accuracy of arcminutes or arcseconds, reducing the probability of chance
79 association.

80 2. HERMES Mission Concept

81 The *High Energy Modular Ensemble of Satellites* (HERMES) project aims
82 to realize a new generation instrument for the observations of high-energy tran-
83 sients. The proposed approach here differs from the conventional idea to build
84 increasingly larger and expensive instruments. The basic HERMES philosophy
85 is to realize innovative, distributed and modular instruments composed by
86 tens/hundreds of simple units, cheaper and with a limited development time.
87 The present nanosatellite (e.g. CubeSats) technologies demonstrates that off-
88 the-shelf components for space use can offer solid readiness at a limited cost.
89 For scientific applications, the physical dimension of a single detector should to
90 be compatible with the nanosatellite structure (e.g. 1U CubeSat of $10\times 10\times 10$
91 cm³). Therefore, the single HERMES detector is of course underperforming
92 (i.e. it has a low effective area), when compared with conventional operative
93 transient monitors, but the lower costs and the distributed concept of the in-
94 strument demonstrate that is feasible to build an innovative instrument with

95 unprecedented sensitivity. The HERMES detector will have a sensitive area
 96 $>50 \text{ cm}^2$, therefore with several tens/hundreds of such units a total sensitive
 97 area of the order of magnitude of $\sim 1 \text{ m}^2$ can be reached.

98 By measuring the time delay between different satellites, the localisation
 99 capability of the whole constellation is directly proportional to the number of
 100 components and inversely proportional to the average baseline between them.
 101 As a rough example, with a reasonable average baseline of $\sim 7000 \text{ km}$ (comparable to the Earth radius, and a reasonable number for low-Earth satellites in suitable orbits) and ~ 100 nanosatellites simultaneously detecting a transient,
 102 a source localisation accuracy of the order of magnitude of $\sim 10 \text{ arcsec}^2$ can be
 103 reached, for transients with short time scale (ms) variability.
 104

105 The current phase of the project, *HERMES Technological Pathfinder* (TP),
 106 focuses on the realization of three nanosatellites, ready for launch at mid-2020.
 107 The purpose here is to demonstrate the feasibility of the HERMES concept,
 108 operating some units in orbit and to detect a few GRBs. The next phase of the
 109 project, *HERMES Scientific Pathfinder* (SP), will demonstrate the feasibility of
 110 GRB localisation using up to 6–8 satellites in orbit. Although in both these preliminary phases reduced ground segment capabilities will be used, i.e. reduced
 111 data-downloading with a few ground contacts/day, the complete development
 112 of the HERMES detectors is expected. These activities will pave the way to the
 113 final HERMES constellation composed of hundreds of nanosatellites. Detailed
 114 mission studies, including orbital configuration, attitude control strategy, and
 115 sensitive area distribution will be performed, as well as a proper planning of
 116 the ground segment allowing to reach the ambitious scientific requirements, i.e.
 117 prompt diffusion of the transient accurate localization. Thanks to the production approach, the context of a typical Small or Medium-class space mission
 118 seems to be compatible with HERMES final constellation, where most of the
 119 resources will be devoted to the multiple launches and to the realization of the
 120

$2\sigma_{\text{pos}} = \sigma_{\text{CCF}}/Bc\sqrt{N(N-1-2)} \approx 10 \text{ arcsec}$; where B is the baseline, N the number of satellites and σ_{CCF} is the error associated with the cross-correlation function.

123 ground segment.

124 **3. Payload Description**

125 A possible solution for the HERMES payload is allocated in 1U-Cubesat
126 ($10 \times 10 \times 10$ cm³), cf. Figure 1. A mechanical support is placed on the in-
127 strument topside. The support is composed by two parts to accommodate an
128 optical/thermal filter in the middle. The electronic boards for the Back-End
129 and the Data Handling unit are allocated on the bottom of the payload unit.
130 The detector core is located in the middle: this is a scintillator-based detector
131 in which Silicon Drift Detectors (SDD, [5]) are used to both detect soft X-rays
132 (by direct absorption in silicon) and to simultaneously readout the scintillation
133 light. The payload unit is expected to allocate a detector with >50 cm² sen-
134 sitive area in the energy range from $3-5$ keV up to 2 MeV, with a total power
135 consumption <4 W and total weight of <1.5 kg.

136 *3.1. Detector core architecture*

137 Aiming at designing a compact instrument with a very wide sensitivity band,
138 the detector is based on the so-called “siswich” concept [3, 4], exploiting the
139 optical coupling of silicon detectors with inorganic scintillators. The detector
140 is composed by an array of scintillator pixels, optically insulated, read out by
141 Silicon Drift Detectors.

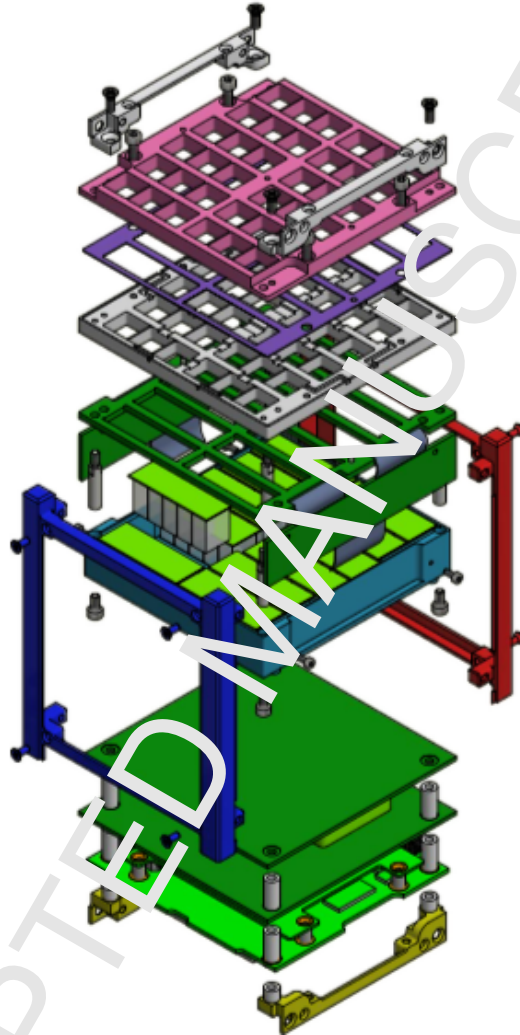


Figure 1: Exploded view of the payload unit ($10 \times 10 \times 10 \text{ cm}^3$) on board the HERMES nanosatellite. From the top are shown the mechanical support composed by top (pink) and bottom (gray) parts, with optical filter (violet) in middle, the FEE board (dark green) allocating SDD matrices (light green), FE-LYRA chips on the top and BE-LYRA chips folded on the side (not shown for clarity), the GAGG crystal pixels (white transparent) and their housing (greenish blue). Mechanical ribs on top (grey) and on bottom (yellow) are also visible, necessary to fix the payload components to the satellite structure (blue and red).

142 In this concept the SDDs play the double role of read-out device for the opti-
 143 cal signal from the scintillator and of an independent X-ray solid state detector.

144 Low energy X-rays are directly absorbed by the SDD, while higher energy X-
 145 rays and γ -rays are absorbed in the crystal and the optical scintillation photons
 146 are collected by the same detector. Only very low noise readout sensors and
 147 front-end electronics allow to reach a low energy scintillator threshold below
 148 20–30 keV. Above these energies the increasing sensitivity of the scintillator is
 149 able to compensate the lack of efficiency of thin silicon sensors (450 μm), so
 150 a quite flat efficiency in a wide energy band for the whole integrated system
 151 is reached. The inorganic scintillators selected for this innovative detector is
 152 the recently developed [6] Cerium-doped Gadolinium-Aluminum-Gallium Gar-
 153 net (Ce:GAGG), a very promising material with all the required characteristics,
 154 i.e. a high light output ($\sim 50,000$ ph/MeV), no internal radioactive background,
 155 no hygroscopicity, a fast radiation decay time of ~ 90 ns, a high density (6.63
 156 g/cm^3), a peak light emission at 520 nm and an effective mean atomic number of
 157 54.4. All these characteristics make this material very suitable for the HERMES
 158 application. Since GAGG is a relatively new material, it has not yet extensively
 159 investigated with respect to radiation resistance and performance after irradi-
 160 ation, although the published results are very encouraging [7–9]. These tests
 161 showed that GAGG has a very good performance, compared to other scintillator
 162 materials largely used in the recent years in space-borne experiments for γ -ray
 163 astronomy (e.g. BGO or CsI), i.e. a very low activation background (down to
 164 2 orders of magnitude lower than BGO), and a minor light output degradation
 165 with accumulated dose.

166 The SDD development builds on the state-of-the-art results achieved within
 167 the framework of the Italian ReDSOX collaboration, with the combined de-
 168 sign and manufacturing technology coming by a strong synergy between INFN-
 169 Trieste and Fondazione Bruno Kessler (FBK, Trento), in which both INFN and
 170 FBK co-fund the production of ReDSOX Silicon sensors. A custom geometry for
 171 a SDD matrix (Figure 2) was designed, in which a single crystal ($\sim 12.1 \times 6.94$
 172 cm^2) is coupled with two SDD channels. Therefore, the scintillator light uni-
 173 formly illuminates two cells, giving rise to a comparable signal output for both
 174 channels. This allows to discriminate scintillator events (higher energy γ -rays)

175 by their multiplicity: lower energy X-rays, directly absorbed in the SDD, are
 176 read out by only one channel.

177 3.2. Readout ASIC: from VEGA to LYRA

178 The HERMES detector, constituted by 120 SDD cells distributed over a total
 179 area of $\sim 92 \text{ cm}^2$, requires a peculiar architecture for the readout electronics.
 180 A low-noise, low-power Application Specific Integrated Circuit (ASIC) named
 181 LYRA has been conceived and designed for this task. LYRA has an heritage
 182 in the VEGA ASIC [10, 11] that was developed by Politecnico of Milano and
 183 University of Pavia within the ReDSOX Collaboration during the LOFT Phase-
 184 A study (ESA M3 Cosmic Vision program), although a specific and renewed
 185 design is necessary to comply with the different SDD specifications, the unique
 186 system architecture and the high signal dynamic range needed for HERMES. A
 187 single LYRA ASIC is conceived to operate as a constellation of 32+1 Integrated
 188 Circuit (IC) chips. The 32 Front-End ICs (FE-LYRA) include preamplifier, first
 189 shaping stage and signal line-transmitter, the single Back-End IC (BE-LYRA)
 190 is a 32-input ASIC including all the circuits to complete the signal processing
 191 chain: signal receiver, second shaping stage, discriminators, peak&hold, control
 192 logic, configuration registers and multiplexer. The FE-LYRA ICs are small
 193 ($0.9 \times 0.6 \text{ mm}^2$ die) allowing to be placed very close to the SDD anodes, in
 194 order to minimize the stray capacitances of the detector-preamplifier connection,
 195 maximizing the effective-to-geometric area ratio ($\sim 54 \text{ cm}^2$ vs. $\sim 92 \text{ cm}^2$). In
 196 this configuration (Figure 2), the BE-LYRA chips ($\sim 6.5 \times 2.5 \text{ mm}^2$ die) can be
 197 placed out of the detection plane, allocating SDD matrix and FE-LYRA ICs
 198 on a rigid part by means of embedded flex cables. The flat cables allow also
 199 avoiding the additional space required by connectors, offering the possibility to
 200 “flip” the boards allocating the BE-LYRA chips (on a rigid part) at right angle
 201 with respect to the detection plane, on the external side of the payload unit.

202 3.3. Back-End Electronics

203 The Back-End electronics (BEE) of HERMES includes the BE-LYRA chips,
 204 external commercial analog-to-digital (ADC) converters and a FPGA-based con-

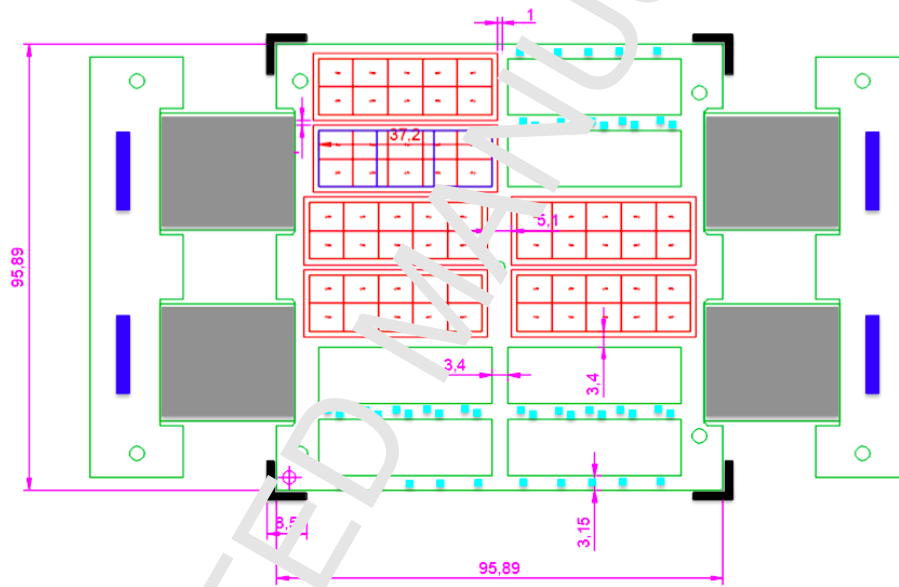


Figure 2: Sketch of the top view of FEE board for the HERMES nanosatellite. The black corner indicate the overall nanosatellite structure ($10 \times 10 \text{ cm}^2$). The board will allocate SDD matrices (in red) and FE-LYRA chips (light blue) very close to each SDD anode. The BE-LYRA chips (blue) are allocated on the rigid part that will be folded on the side of the satellite, by means of flex cables (gray).

205 trol logic. The control logic takes care of the signal handshake required to
206 read out analogue signals from BE-LYRA chips, synchronizing the digital conver-
207 sion operations, and time tagging the events based on conventional GPS sensor,
208 combining an atomic clock signal (CSAC) to reduce as much as possible the
209 natural shift/jitter of the GPS sensor ensuring a sub-microsecond timing reso-
210 lution. Due to the peculiar architecture of the detector core, the BEE will also
211 perform the Event Data Generator functionality: automatically discriminating
212 the location of photon interaction (silicon or scintillator), on the basis of the
213 multiplicity of the readout signals. This fundamental task has to be carried
214 out in real-time to generate the photon lists that include channel address, time
215 of arrival of photons and a raw energy estimation, which are mandatory for
216 scientific data processing based on a suitable on-board logic.

217 *3.4. Payload Data Handling Unit*

218 The HERMES Payload Data Handling Unit (PDHU) will be implemented on
219 iOBC, manufactured by ISIS, a commercial on-board computer. This model,
220 with a weight of ~ 100 g and an average power consumption of 400 mW, will im-
221 plement all functionalities required for HERMES, such as telecommands (TCs),
222 housekeeping (HKs), power system commanding (PSU), handling operative
223 modes of the payload (by TCs or automatically), generating the telemetry pack-
224 ets (TMs) and managing the interface with the spacecraft. A custom algorithm
225 making the satellites sensitive X-ray and γ -ray transients, continuously compare
226 the current data rate of the instrument with the average background data rate
227 taken previously. When a transient occurs, the events, recorded on a circular
228 buffer, are then sent to the ground on telemetry packets. Due to the different
229 families of GRB, ratemeters on different timescales, energy bands and different
230 geometric regions of the detection plane will be implemented.

231 **4. Conclusion**

232 The HERMES project final aim is to realize a new generation instrument
233 composed by hundreds of detectors onboard nanosatellites. This disruptive tech-

234 nology approach, although based on “underperforming” individual units, allows
235 to reach overall sensitive areas of the order of $\sim 1 \text{ m}^2$, with unprecedented scientific
236 performance for the study of high-energy transients such as GRBs and gravitational
237 wave counterparts. The current ongoing phase of the HERMES project
238 (Technological Pathfinder), focuses on the realization of the three nanosatellites
239 to be launched in mid-2020, that will demonstrate the proposed approach to
240 detector design (Silicon Drift Detectors coupled to GAGG:Ce scintillator crystals)
241 and its performance. In this framework, relevant prototyping activities are
242 currently under development, towards the implementation phase.

243 Acknowledgments

244 HERMES is a *Progetto Premiale MUR*. The authors acknowledge INFN
245 and FBK (RedSoX2 project and FFK-INFN agreement 2015-03-06), ASI and
246 INAF (agreements ASI-UNI-Ca 2016-10-U.O and ASI-INAF 2018-10-hh.0).

247 References

- 248 [1] R.W. Klebesadel et al., *Astrophysical Journal*, v. 182 (1973) L85
- 249 [2] B.P. Abbott et al., *The Astrophysical Journal Letters*, v. 848 (2017) L12
- 250 [3] M. Marisaldi et al., *Nucl. Instrum. Meth. A*, v. 588 (2008) 37–40
- 251 [4] M. Marisaldi et al., *IEEE Trans. Nucl. Sci.*, v. 51 (2004) 1916
- 252 [5] E. Catt and P. Rehak, *Nucl. Instrum. Meth. in Physics Research*, v. 225
253 (1984) 600–614
- 254 [6] K. Kawada, et al., *IEEE Trans. Nucl. Sci.*, v. 59, (2012) 2112 – 2115
- 255 [7] M. Sakano, et al., *Journal of Instr.*, v. 9 (2014) P10003
- 256 [8] T. Yanagida, et al., *Optical Materials*, v. 36 (2014) 2016 – 2019
- 257 [9] M. Yoneyama, et al., *Journal of Instr.*, v. 13 (2018) P02023

- 258 [10] M. Ahangarianabhari, et al., Journal of Instr., v. 9 (2014) C03036
- 259 [11] R. Campana, et al., Journal of Instr., v. 9 (2014) P08008

ACCEPTED MANUSCRIPT